

## Interpretation of the photoluminescence spectrum of double quantum rings

Tommy Vänskä\* and Dage Sundholm†

Department of Chemistry, University of Helsinki, P.O. Box 55 (A.I. Virtanens plats 1), FIN-00014 Helsinki, Finland

(Received 11 May 2010; revised manuscript received 17 June 2010; published 4 August 2010)

We present accurate configuration-interaction calculations of energy levels and radiative recombination rates for excitonic systems confined in concentric double quantum rings. The calculations yielded three exciton states that can contribute to the observed photoluminescence spectra. The simulated photoluminescence spectra are in excellent agreement with the observed ones. The three bright states were found to be confined into the inner ring. Thus, the calculations do not support the accepted notion that the coupling between the bright states is weak because they are spatially separated. Instead, we propose that the two nearly degenerate upper states are giving rise to the high-energy peak of the experimental photoluminescence spectra of the double quantum rings. The two bright excited states have significant population because the exciton is trapped there due to phonon-bottleneck effects.

DOI: [10.1103/PhysRevB.82.085306](https://doi.org/10.1103/PhysRevB.82.085306)

PACS number(s): 73.21.La, 31.15.V-, 71.35.-y, 78.60.-b

### I. INTRODUCTION

Semiconductor quantum dots and related structures, such as concentric quantum rings (CQRs), are of great interest due to their optoelectronic properties and corresponding potential as building blocks for nanoscale devices.<sup>1-5</sup> A thorough understanding of their electronic structure and carrier recombination dynamics is thus called for. The excitons trapped in a quantum-dot structure consist of a strongly interacting electron-hole pair. It is therefore of interest to study the effects of correlation on the properties of these structures.<sup>6</sup>

We have developed an *ab initio* program package for studies of electron-hole pairs confined in semiconductor quantum dot and quantum ring structures. The computational methods are based on configuration-interaction (CI) and coupled-cluster (CC) approaches,<sup>7,8</sup> which can utilize all or a subspace of the symmetry-adapted many-body states obtained by distributing the electrons and holes among the one-particle states. The calculations reported here employ the CI method, which when utilizing the complete many-body space (full CI or FCI) is equivalent to exact diagonalization.

In this paper we present the results of FCI calculations on excitons and multiexcitons confined in a concentric double quantum ring (CDQR) structure. The low part of the energy spectrum is calculated and the corresponding states examined through the one-body densities. The radiative recombination rates for the exciton and biexciton are also calculated. The transition rates do not, of course, constitute a complete description of the photoluminescence (PL). A rigorous model would need to examine the entire process from excitation in the substrate and subsequent intraband relaxation pathways in order to describe how the luminescent states are populated as a function of time. Nevertheless, since the PL intensity is directly proportional to the transition rates we will compare our results with experimental PL spectra and previous theoretical treatments.

### II. MODEL

The implemented CI model is based on the effective-mass approximation (EMA), which is expected to be valid for the

system studied here.<sup>9-12</sup> To keep the model simple we neglect the heavy-hole (HH) and light-hole band mixing and consider only the HH band. Utilizing the full configuration space spanned by the basis set, the exact solution of the effective-mass Schrödinger equation is obtained, within the limits of the chosen one-particle basis set. FCI represents the top of a hierarchy of CI approximations in which the computational many-body space is generated by “exciting” particles from a reference state, commonly the Hartree-Fock state. By removing at most  $M$  particles from the reference state and permuting them among the unoccupied single-particle states a truncated many-body space is obtained. For  $M=2$  the model is thus called “all singles and doubles CI,” abbreviated CISD, for  $M=3$  triple excitations are included, which is denoted CISDT and so on.

To solve the many-body Schrödinger equation the single-particle states of the electrons and holes are expanded in a Gaussian basis set of the form  $x^{l_x}y^{l_y}z^{l_z}e^{-\alpha(x^2+y^2)}e^{-\beta z^2}$ , where we denote the basis functions with  $l_x+l_y+l_z=0,1,2,\dots$  by the letters  $s,p,d,\dots$ . The different exponents for the  $xy$  plane and the  $z$ -direction stem from the cylindrical symmetry of the confinement potential. The eigenstates may thus be labeled by the total angular momentum  $L_z=L_z^e+L_z^h$ , where the states  $|L_z|=0,1,2,\dots$  will be denoted  $\Sigma,\Pi,\Delta,\dots$ . The width of the rectangular confinement potential in the  $z$  direction is 8 nm and is sufficiently strong to allow us to use basis sets with only one  $s$  function describing the  $z$  dependency of the states.<sup>7,13</sup> The  $\beta$  exponent is optimized at the one-particle level for the employed potential in the  $z$  direction.<sup>14</sup> For the lateral part of the wave functions, we employ an even-tempered basis set consisting of  $8s$ ,  $7p$ , and  $5d$  functions. Studies using different sizes of the basis sets showed that the  $8s7p5d$  set yields converged energies for the studied exciton states. The lateral confinement potential in our model is based on an atomic force microscope profile obtained from a CDQR sample.<sup>15</sup> The confinement potential has the same form as the profile with the minima normalized to 91.9 eV for the electrons and 25.9 eV for the holes. The effective masses used in our calculations are  $m_{xy}^e=m_z^e=0.065$ ,  $m_{xy}^h=0.143$ , and  $m_z^h=0.341$ .<sup>16</sup> The relative dielectric constant is 13.

In the EMA framework, the spontaneous photoemission rate  $\Gamma_{N-1, \mathcal{L} \leftarrow N, \mathcal{R}}$ , for the transition from the right ( $\mathcal{R}$ )  $N$ -exciton state  $|N, \mathcal{R}\rangle$  into the left ( $\mathcal{L}$ )  $(N-1)$ -exciton state  $|N-1, \mathcal{L}\rangle$ , can be written as<sup>16-24</sup>

$$\Gamma_{N-1, \mathcal{L} \leftarrow N, \mathcal{R}} = \frac{ne^2 E_p E_{ph}}{6\pi\hbar^2 c^3 \epsilon_0 m} \sum_{\sigma} |\langle \mathcal{L}, N-1 | P_{\sigma}^{-} | N, \mathcal{R} \rangle|^2, \quad (1)$$

where  $n$  is the refractive index of the semiconductor,  $E_p$  is the Kane matrix element,<sup>25</sup> and  $E_{ph}$  is the emitted photon energy. The operator  $P_{\sigma}^{-}$  is the interband polarization operator<sup>9</sup> which annihilates an electron-hole pair with a given spin projection ( $\sigma = \uparrow$  or  $\downarrow$ ) by creating a photon with a definite circular polarization. By introducing the CI expansions of the  $\mathcal{L}$  and  $\mathcal{R}$  states and simplifying the expression one obtains

$$\Gamma_{N-1, \mathcal{L} \leftarrow N, \mathcal{R}} = \frac{ne^2 E_p E_{ph}}{6\pi\hbar^2 c^3 \epsilon_0 m} \sum_{\sigma} \left| \sum_{ir} \gamma_{ir, \mathcal{L}\mathcal{R}}^{\sigma, -\sigma} \langle i|r \rangle \right|^2. \quad (2)$$

The radiative recombination rate is proportional to the overlap between the one-particle electron and hole functions multiplied by the corresponding element of the recombination density matrix  $\gamma_{ir, \mathcal{L}\mathcal{R}}^{\sigma, -\sigma}$ , which is obtained from the CI coefficients of the  $\mathcal{L}$  and  $\mathcal{R}$  states,

$$\gamma_{ir, \mathcal{L}\mathcal{R}}^{\sigma, -\sigma} = \langle \mathcal{L}, N-1 | c_i d_r | N, \mathcal{R} \rangle = \sum_I C_I^{N-1, \mathcal{L}} C_{I_r}^{N, \mathcal{R}}. \quad (3)$$

The matrix elements of  $\gamma$  contain the many-body information about transitions between states with different numbers of charge carriers, and  $c$  and  $d$  denote annihilation operators for electrons and holes, respectively. The summation in Eq. (3) includes all configurations of the  $|\mathcal{L}, N-1\rangle$  state (with expansion coefficients  $C_I^{N-1, \mathcal{L}}$ ) and  $C_{I_r}$  denotes the CI coefficients of the  $|N, \mathcal{R}\rangle$  state that give a nonvanishing contribution when the electron in spin orbital  $i$  and the hole in spin orbital  $r$  are annihilated.<sup>26</sup>

It is worth noting that symmetry considerations impose restrictions on the states involved in radiative recombination. For example, in the case of one exciton recombining to the vacuum the requirement is that the initial state belongs to the total symmetric irreducible representation ( $\Sigma$ ).

### III. RESULTS

To compare our model with the experimental photoluminescence spectra obtained for CDQR's,<sup>27-29</sup> we solve the FCI problem for a system consisting of one exciton in a CDQR confinement potential whose radial form is shown in Figs. 1 and 2. The densities in Fig. 1(a) are obtained by solving a single-particle model with no charge-carrier interactions. At the one-particle level, one of the two lowest states is centered on the inner and the other on the outer ring (OR), both for the electron and the hole. This is in qualitative agreement with the calculations by Kuroda *et al.*,<sup>28</sup> where a single-particle effective-mass model is used to calculate the one-body electron and hole states of the system. However, we find the lowest-lying state localized in the inner ring and the second lowest in the outer one, whereas Kuroda *et al.* ob-

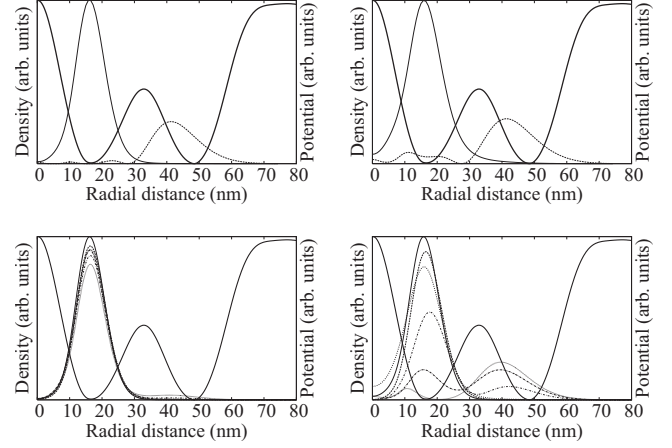


FIG. 1. (a) Electron (left) and hole (right) densities obtained from a single-particle model. (b) FCI densities for the electron (left) and hole (right) part of the exciton. The six lowest lying  $\Sigma$  states are shown.

tained the opposite. All densities are plotted for  $z=0$ .

In contrast, the corresponding FCI densities shown in Figs. 1(b) and 2, do not have any states mainly localized in the outer ring, at least not among the six energetically lowest-lying states in each of the irreducible representations of the symmetry group. Some states do indeed have a considerable density in the outer-ring region, but the  $\Pi$  and  $\Delta$  states, shown in Fig. 2, do not contribute to the luminescence due to symmetry reasons. Some of the dark  $\Sigma$  states are the second component of the corresponding  $\Delta$  state with  $|L_z|=2$ . While states with densities concentrated in the outer ring may well exist they will correspond to energies too high to contribute to the experimental PL spectrum.

We have also performed test calculations using confinement potentials with a higher barrier separating the inner and outer ring without obtaining any significant changes in the character of the lowest states. Different basis-set sizes were also employed. Only by filling the inner minimum of the potential, yielding a single ring, did we find the lowest states localized in the outer-ring region, which also shows that the basis set is, indeed, capable of describing such states.

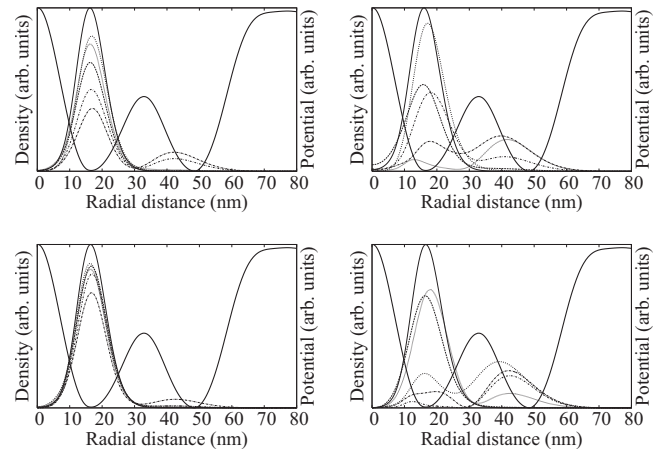


FIG. 2. FCI densities for the six lowest lying (a)  $\Pi$  and (b)  $\Delta$  states for the electron (left) and hole (right) part of the exciton.

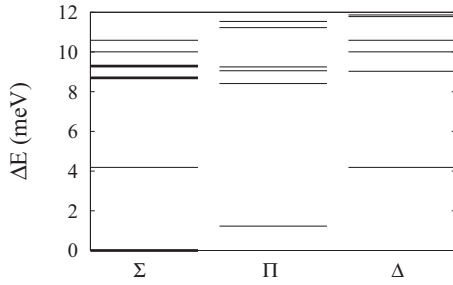


FIG. 3. Low part of the energy spectrum for the exciton.

The low-energy part of the spectrum for the exciton is shown in Fig. 3. The three luminescent  $\Sigma$  states are highlighted with thick lines. Several dark states are present, including one lying between the ground state and the two luminescent excited states.

The importance of charge-carrier correlation in the system can be seen by examining the chemical potential for multi-exciton complexes  $\mu(N) = E_g(N) - E_g(N-1)$ , where  $E_g(N)$  is the ground-state energy for the  $N$ -exciton system. Figure 4 shows  $\mu(N)$  for 1–6 excitons, revealing a shell-like structure [Fig. 4(c)], similar to the one found for “ordinary” quantum dots. The spacing of around 1 meV between the shells, however, is very small compared to the quantum-dot case, which typically has an energy difference on the order of 10 meV between the  $\sigma$  and  $\pi$  shells.<sup>30</sup> The importance of correlation between the charge carriers is clearly seen. Figures 4(a) and 4(b) show  $\mu(N)$  obtained at the CISD and CISDT levels, respectively. At these lower correlation levels the shell structure is not present and the biexciton is not bound. Indeed, quadruple excitations in the CI scheme are needed in order to obtain what we assume to be correct qualitative picture. This behavior is expected based on previous calculations on single-quantum rings, which showed that correlation effects are considerably larger in quantum rings than for quantum dots.<sup>8</sup>

Figure 5 shows the radiative recombination rates for the exciton (1X) and biexciton (2X), calculated within the FCI

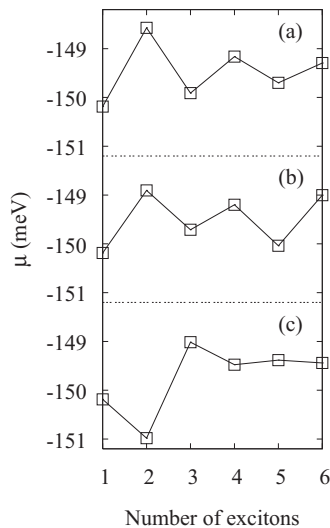


FIG. 4. Chemical potential for the double ring structure obtained from a (a) CISD, (b) CISDT, and (c) CISDTQ (quadruple excitations included) calculation.

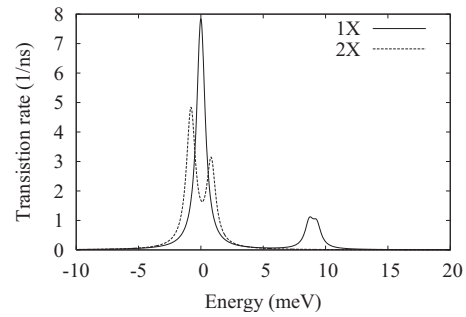


FIG. 5. Radiative recombination rates for 1X and 2X. The energy is expressed relative to the low-energy peak. Lorentzian broadening of the peaks has been employed.

scheme using the expression in Eq. (2). The low-energy peak contains contributions from the recombination of the ground-state exciton as well as from the biexciton. The other peak, lying some 9 meV higher in energy contains contributions from the biexciton and from one or two of the lowest bright excited states of the exciton.

#### IV. DISCUSSION

Several photoluminescence experiments on CDQR structures have been carried out.<sup>27–29</sup> These structures were obtained by a droplet-epitaxial technique, in which GaAs droplets are formed on a  $\text{Al}_x\text{Ga}_{1-x}\text{As}$  substrate, usually with  $x = 0.3$ .<sup>29</sup> Typically, the photoluminescence spectra of the concentric quantum double rings exhibit two main peaks, the characteristics of which have been suggested to indicate that they correspond to recombination from states localized on the inner ring (IR) and OR of the CDQR sample. The calculations presented above, which are exact in the limit of the complete single-particle basis, do not support the existence of low-lying and luminescent OR states. However, the main features of the experimental PL are nevertheless reproduced by considering the electron-hole recombination from the ground state and the first excited states of the exciton that has a significant photoemission probability. The excited state can be expected to have a long enough lifetime due to phonon-bottleneck effects.<sup>16,31,32</sup> The bottleneck should be more prominent in a ring structure as compared to a quantum dot, due to the shape of the wave functions involved; the maximum of potential of the CQR structures in the origin leads to states which are more extended in real space, corresponding to a narrower distribution in momentum space, which impairs phonon-mediated relaxation.

In their experimental studies of the PL spectra of the CDQR's, Sanguinetti *et al.*<sup>27</sup> noticed that the populations of the states responsible for the two peaks in the luminescence spectra were independent and concluded that the recombination kinetics of the states of the luminescence peaks was decoupled. Their calculations of single-particle electron and hole states suggested that the lowest state is located in the outer ring and the second one lies in the inner ring. They suggested that the spatial separation of the states into the two wells makes independent recombination processes feasible. This conclusion was supported by their high-intensity exci-

tation experiments, which showed that in the cascade-type dynamics, higher excited states function as feeders to the lower-lying luminescent states. However, this is not the only possible interpretation of the observations. The present FCI calculations yielded three luminescent states. The ground state and two almost degenerate states lying about 9 meV higher in energy. The relative positions of the peaks in calculated photoluminescence spectrum agree well with experiment.<sup>27,28</sup> Our calculations show that all three luminescent states are mainly located in the inner ring, indicating that the previously suggested recombination mechanism is not completely correct. The attractive Coulomb interaction between the charge carriers of the excitons stabilizes the IR states more than the OR ones because they have a shorter average distance between the electrons and the holes than the OR states. Even though the upper and lower bright states are located in the same potential well and the population of the upper states are maintained by phonon-bottleneck effects, the bright ground state can be populated from higher excited

states along relaxation paths that do not significantly involve the upper luminescent states. Figure 3 shows that there are many excited states with about the same energy as the upper bright states implying that the energy transfer via a cascade mechanism is feasible also without involving the upper bright states. Nothing prevents the excitons from being trapped in the upper bright states long enough to render electron-hole recombination feasible and without significantly affecting the population of the bright ground state.

#### ACKNOWLEDGMENTS

This research has been supported by the Academy of Finland through its Centers of Excellence Programme 2006–2011 and the OPNA research project (Grant No. 118195). Financial support from the Magnus Ehrnrooth foundation is also acknowledged. We would also like to thank Stefano Sanguinetti for providing the AFM profile and valuable comments and discussion.

\*FAX: +358-9 191 50169; tommy@chem.helsinki.fi

†sundholm@chem.helsinki.fi

<sup>1</sup>O. Voskoboynikov, Y. Li, H.-M. Lu, C.-F. Shih, and C. P. Lee, *Phys. Rev. B* **66**, 155306 (2002).

<sup>2</sup>J. I. Climente, J. Planelles, and J. L. Movilla, *Phys. Rev. B* **70**, 081301 (2004).

<sup>3</sup>J. A. Barker, R. J. Warburton, and E. P. O'Reilly, *Phys. Rev. B* **69**, 035327 (2004).

<sup>4</sup>R. J. Warburton, C. Schäflein, D. Haft, F. Bickel, A. Lorke, K. Karrai, J. M. Garcia, W. Schoenfeld, and P. M. Petroff, *Nature (London)* **405**, 926 (2000).

<sup>5</sup>A. Lorke, R. J. Luyken, A. O. Govorov, J. P. Kotthaus, J. M. Garcia, and P. M. Petroff, *Phys. Rev. Lett.* **84**, 2223 (2000).

<sup>6</sup>F. Boxberg and J. Tulkki, *Rep. Prog. Phys.* **70**, 1425 (2007).

<sup>7</sup>T. Vänskä, M. Lindberg, J. Olsen, and D. Sundholm, *Phys. Status Solidi B* **243**, 4035 (2006); QDOT is a configuration-interaction and coupled-cluster program for semiconductor quantum dots authored by M. Braskén, S. Corni, M. Lindberg, J. Olsen, D. Sundholm, and T. Vänskä.

<sup>8</sup>O. Lehtonen, D. Sundholm, and T. Vänskä, *Phys. Chem. Chem. Phys.* **10**, 4535 (2008).

<sup>9</sup>L. Jacak, P. Hawrylak, and A. Wojs, *Quantum Dots* (Springer, Berlin, 1998).

<sup>10</sup>A. W. Wojs, P. Hawrylak, S. Fafard, and L. Jacak, *Phys. Rev. B* **54**, 5604 (1996).

<sup>11</sup>P. Hawrylak, *Phys. Rev. B* **60**, 5597 (1999).

<sup>12</sup>A. Franceschetti and A. Zunger, *Phys. Rev. Lett.* **78**, 915 (1997).

<sup>13</sup>J. Tulkki and A. Heinämäki, *Phys. Rev. B* **52**, 8239 (1995).

<sup>14</sup>M. Braskén, M. Lindberg, D. Sundholm, and J. Olsen, in *Conference Proceedings: Atoms, Molecules and Quantum Dots in Laser Fields: Fundamental Processes*, edited by N. Bloembergen, N. Rahman, and A. Rizzo (Societa' Italiana di Fisica, Bologna, 2001), Vol. 71, pp. 315–324.

<sup>15</sup>S. Sanguinetti (private communication).

<sup>16</sup>M. Braskén, S. Corni, M. Lindberg, J. Olsen, and D. Sundholm,

*Mol. Phys.* **100**, 911 (2002).

<sup>17</sup>R. H. Haug and S. W. Koch, *Quantum Theory of the Optical and Electronic Properties of Semiconductors* (World Scientific, Singapore, 1990).

<sup>18</sup>G. Bastard, *Wave Mechanics Applied to Semiconductor Heterostructures* (Les Editions de Physique, Les Ulis, 1988).

<sup>19</sup>D. Bimberg, M. Grundmann, and N. Ledentsov, *Quantum Dot Heterostructures* (Wiley, New York, 1999).

<sup>20</sup>T. Wenckebach, *Essentials of Semiconductor Physics* (Wiley, Chichester, 1999).

<sup>21</sup>T. Feldtmann, L. Schneebeli, M. Kira, and S. W. Koch, *Phys. Rev. B* **73**, 155319 (2006).

<sup>22</sup>P. A. Dalgarno, J. M. Smith, J. McFarlane, B. D. Gerardot, K. Karrai, A. Badolato, P. M. Petroff, and R. J. Warburton, *Phys. Rev. B* **77**, 245311 (2008).

<sup>23</sup>M. Wimmer, S. V. Nair, and J. Shumway, *Phys. Rev. B* **73**, 165305 (2006).

<sup>24</sup>G. A. Narvaez, G. Bester, and A. Zunger, *Phys. Rev. B* **72**, 245318 (2005).

<sup>25</sup>J. Singh, *Physics of Semiconductors and their Heterostructures* (McGraw-Hill, New York, 1993).

<sup>26</sup>S. Corni, M. Braskén, M. Lindberg, J. Olsen, and D. Sundholm, *Phys. Rev. B* **67**, 085314 (2003).

<sup>27</sup>S. Sanguinetti, M. Abbarchi, A. Vinattieri, M. Zamfirescu, M. Gurioli, T. Mano, T. Kuroda, and N. Koguchi, *Phys. Rev. B* **77**, 125404 (2008).

<sup>28</sup>T. Kuroda, T. Mano, T. Ochiai, S. Sanguinetti, K. Sakoda, G. Kido, and N. Koguchi, *Phys. Rev. B* **72**, 205301 (2005).

<sup>29</sup>T. Mano *et al.*, *Nano Lett.* **5**, 425 (2005).

<sup>30</sup>M. Braskén, M. Lindberg, D. Sundholm, and J. Olsen, *Phys. Rev. B* **61**, 7652 (2000).

<sup>31</sup>U. Bockelmann, *Phys. Rev. B* **48**, 17637 (1993).

<sup>32</sup>A. Bertoni, M. Rontani, G. Goldoni, and E. Molinari, *Phys. Rev. Lett.* **95**, 066806 (2005).